A Metaheuristic-Based Methodology to Minimize the Concentration of Lateral Displacements in Low-Rise Steel Concentrically Braced Frames Subjected to Seismic Loading

Bardia Mahmoudi and Ali Imanpour

Abstract This paper proposes a new methodology to evaluate the seismic performance of multi-storey Concentrically Braced Frames (CBFs) and to minimize the concentration of frame nonlinear lateral displacements. A three-storey concentrically braced frame with chevron bracing is first selected. An optimization tool is then developed to study drift concentration under seismic loading. This tool leverages a fully parametric design script interacting with the *OpenSees* programme to generate a large number of potential frame designs analysed under ground motion accelerations and to iteratively update the frame design using the PSO algorithm until minimum drift concentration is achieved. Preliminary results of the proposed methodology and future direction of the research are finally presented.

Keywords Lateral displacements · Low-rise steel concentrically braced frames · Seismic response

1 Introduction

Steel Concentrically Braced Frames (CBFs) are widely used as the lateral load-resisting system of multi-storey buildings. Under lateral seismic loads, the lateral roof displacement may not be distributed evenly between the storeys as their braces experience nonlinear response through tensile yielding and buckling, resulting in the concentration of lateral inelastic displacements in one or some of the storeys. This stems from a poor performance of CBFs in redistributing inelastic demands along their height mainly due to inherent poor hysteretic response of diagonal braces when buckling in compression, which significantly reduces storey shear resistance, thus

B. Mahmoudi (✉) · A. Imanpour
Department of Civil and Environmental Engineering, University of Alberta, Edmonton, AB, Canada
e-mail: bardia1@ualberta.ca

R. Gupta et al. (eds.), *Proceedings of the Canadian Society of Civil Engineering Annual Conference 2022*, Lecture Notes in Civil Engineering 348,
https://doi.org/10.1007/978-3-031-34159-5_13

discouraging yielding to develop in adjacent floors [20, 29, 32, 54, 60]. This response is compared to an ideal uniform lateral displacement response in Fig. 1 for a three-storey steel CBF with chevron bracing. As shown in Fig. 1a, a desirable response involves brace tensile yielding and compression buckling in all the storeys, resulting in a uniform distribution of lateral displacements over the height of the frame, whereas the frame in real-life under earthquake loading may experience concentration of lateral deformation as shown in Fig. 1b (e.g. in the first storey) due to the elastic response of tension-acting braces in some of the storeys (e.g. Storeys 2 and 3), leading to soft or weak storey behaviour. The concentration of lateral deformations become more critical in tall CBFs, those with heavy gravity loads imposing large P-Δ effects, and the CBFs located in high seismic regions such as Vancouver or Victoria, BC [28, 44, 53, 56].

Several design parameters can influence the distribution of the lateral frame displacement under seismic loads. Past numerical studies have shown the number of storeys, distribution of seismic mass along the frame height, column orientation and splices, brace demand-to-capacity ratios, lateral stiffness offered by adjacent gravity columns, bracing configuration (e.g. X-bracing, chevron, diagonal), bracing system (e.g. tension–compression, tension-only), brace slenderness ratio within each storey and its variation over the storeys can affect seismic behaviour of concentrically braced frames [28, 52, 54].

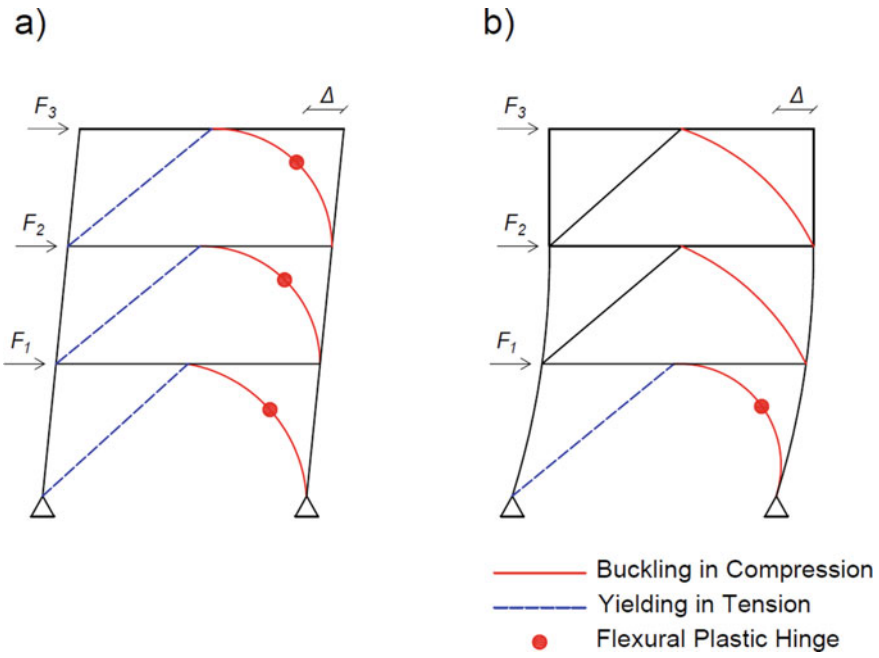

Fig. 1 Comparison of concentrically braced frames lateral deformation distributions: **a** uniform lateral deformation distribution, **b** damage concentration in storey 1

A number of mitigation techniques have been evaluated and proposed by various researchers in the past to reduce the concentration of lateral deformations in steel CBFs. These techniques include (1) rigid truss or strong-back systems tied to the CBF where the CBF acts as the energy dissipation system and the rigid truss is intended to remain essentially elastic forcing the CBF to undergo uniform lateral deformations during inelastic response [14, 33–35, 43, 54–56, 62], (2) innovative bracing members such as buckling-restrained braces (BRBs) instead of conventional braces [2, 3, 12, 19, 21, 26, 27, 38, 45–47, 51, 57, 59, 61], (3) moment-resisting frame (MRF) used in addition to the CBF to engage frame action [13, 16, 25, 62], (4) zipper or vertical tie bar systems [24, 49, 66], (5) two-storey X (split-X) system aiming at developing a 2-storey collapse mechanism [54], (6) rocking systems [4, 18, 22, 37, 41, 48, 58, 63, 64, 7–9, 30, 42, 65].

An alternative design solution to tackle damage concentration in CBFs and achieve a more uniform seismic response is to adjust brace selection, in particular, the brace slenderness parameter $\lambda = KL/r(F_y/\pi^2 E)^{1/2}$ where K is the effective length factor, L is the brace length, r is the radius of gyration of the brace cross-section, F_y is the steel yield stress, and E is Young's modulus of steel. Lacerte and Tremblay [28] developed a method for the selection of braces in Split-X concentrically braced frames such that they attain smooth variations of the post-buckling shear resistance over the frame height. In this method, braces having relatively low slenderness and post-buckling resistance were selected to help the propagation of inelastic deformations in several storeys under major seismic events producing a large lateral displacement at the roof level (in the order of 2% roof drift). This method was verified for systems up to 12 storeys and showed that it can avoid soft storey mechanisms and achieve more stable global response. Drift concentration in 1–8 storey X-braced frames designed as tension–compression or tension-only system was mitigated by limiting brace slenderness to 2.65 and designing the columns for an in-plane demand equal to 20% of the plastic moment capacity of the section in addition to the axial compression forces arising from brace axial resistances and gravity loads [52]. Imanpour et al. [20] proposed a design method for multi-tiered concentrically braced frames experiencing significant drift concentration in one of the braced tiers under seismic-induced deformation demands, leading to column yielding and instability. The method involved new strength and stiffness requirements for columns, which engage column flexural stiffness to force tensile yielding in adjacent braces under seismic loading.

Although various approaches have been proposed in the past to tackle the poor seismic performance of steel CBFs when it comes to the distribution of nonlinear lateral deformations over the frame height and reducing CBF vulnerability to damage concentration and dynamic instability, they lack taking into account inclusive design parameters (e.g. number of storeys, brace slenderness ratio, column orientation, brace demand-to-capacity ratios, bracing configuration and system) affecting the seismic response of CBFs. To this end, this study proposes and implements a metaheuristic optimization tool to overcome the challenges associated with investigating the influence of various design scenarios, which can become computationally intensive, and to develop a design strategy to efficiently achieve a uniform distribution of lateral inelastic deformations under seismic loading. The proposed optimization tool is

developed by linking a fully parametric numerical model of multi-storey CBF, a three-storey chevron braced frame presented in this paper, to the optimization algorithm, which generates a large number of potential frames by varying the influential parameters pertaining to brace design and then updates each frame's members until damage concentration is minimized. This results in a number of candidate frame designs, which are subsequently classified into a small number of groups as final design alternatives using clustering algorithms.

2 Research Methodology

To measure and evaluate concentration of lateral deformation in CBFs, the Drift Concentration Ratio (DCR) is defined as the maximum standard deviation of storey drifts recorded under a given ground motion record. The frame that possesses the smallest DCR is then considered as the one achieving a nearly uniform distribution of lateral displacements over the height. However, finding the frame with the minimum DCR in a large set of frames generated to evaluate damage concentration would be a challenging task if traditional mathematical methods, which require computing derivatives of a function with respect to its variables, were to be used because the DCR cannot be expressed as a continuous and differentiable function of the design variables or the loading input, e.g. ground motion acceleration. Metaheuristic optimization algorithms, which have been developed based on evolutionary behaviour of species in nature, can be implemented instead [50]. The essence of such methods lies on their capability to locate global optimum of a function just by evaluating its value at different points over function's domain, which in the context of this study can help assess design parameter patterns in CBFs, contributing to a better understanding and quantification of such parameters and their impact on minimizing the concentration of frame lateral nonlinear deformations. The Particle Swarm Optimization (PSO) algorithm [23], which is a single objective metaheuristic optimization algorithm vastly used in various engineering disciplines, will be exploited in this study to overcome the challenge of finding the CBF design with the minimum DCR by bypassing a more complex assessment involving the combination of a large number of design variables. The key steps of the iterative process adopted here to minimize the objective function, i.e. the DCR, with respect to its variables, i.e. brace cross-sections, taking advantage of the PSO algorithm are summarized below:

1. *Generate random population*: A set of random particles with a population of N, i.e. first generation, is created by assigning random values to variables associated with the problem. Each particle returns a specific value for the objective function defined for the optimization problem and by inspecting these values, different particles can be ranked against each other.
2. *Objective function evaluation*: Particles defined in Step 1 are subject to various constraints with a feasible space. The selected algorithm forces these constraints to the particles using a penalty function. If a particle satisfies all the constraints,

the value of its objective function remains the same. Otherwise, the particle would get penalized by a multiplier implicit in its objective function to increase its value such that it cannot compete with feasible solutions of the generation when they are ranked based on their objective function.

3. *Particle updating by adjusting their velocity*: Once the set is sorted in accordance with the particle objective functions, the algorithm updates particles inside the generation by adjusting their variables using a velocity term v leading to a new set of solutions, i.e. the next generation. The algorithm then attempts to find the objective function's global minimum by generating a new set of particles and guiding them towards the global optimum. To update the location of particle i in generation t, x_i^t, and obtain the adjusted location in generation $t+1$, x_i^{t+1}, using the velocity parameter v_i^{t+1}, Eqs. 1 and 2 can be used as follows:

$$x_i^{t+1} = x_i^t + v_i^{t+1} \tag{1}$$

$$v_i^{t+1} = wv_i^t + c_1 r_1 \left(x_{pb}^t - x_i^t\right) + c_2 r_2 \left(x_{gb}^t - x_i^t\right) \tag{2}$$

where inertia factor w and trust constants c_1 and c_2 are selected depending on the optimization problem and determine whether the particle should move towards its local best record or the global best record [40]. Factors r_1 and r_2 take random values between 0 and 1 in each iteration, which helps formulate randomness within the algorithm and search the entire feasible domain of the problem instead of getting trapped in local optima zones. It is recommended to set $w = 0.7298$ and $c_1 = c_2 = 1.4962$ in order to improve the algorithm's convergence rate [10]. It is worth noting that v_i^t can be taken as zero in the first generation.

A particle's velocity is a function of three parameters, (1) its velocity in the previous generation, v_i^t, (2) the location of personal best of that particle, x_{pb}^t, representing the coordinate in which particle i has recorded the smallest value it could obtain for the objective function after being modified for t generations, and (3) the location of global best, x_{pb}^t, being the coordinate of the smallest value achieved for the objective function by comparing the results of all particles after t generations. Figure 2 shows the interaction between these three parameters.

4. *Approaching optimum solution*: As Steps 2 and 3 are repeated, the algorithm tries to find the best solutions of each generation and improves them in subsequent generations. This process eventually converges to the optimum solution provided that a sufficient number of iterations are conducted. The algorithm should then terminate creating new generations and bypass performing Steps 2 and 3 by either setting a total number of generations before the algorithm started generating solutions, or verifying the convergence at each iteration by comparing the best solutions of the last two generations with each other (if the difference between the objective function values corresponding to these two solutions is less than the specified tolerance it means the algorithm can no longer find a more optimal solution and it should stop generating new solutions). The drawback associated with the latter is that the algorithm may get stuck around a local optimum and

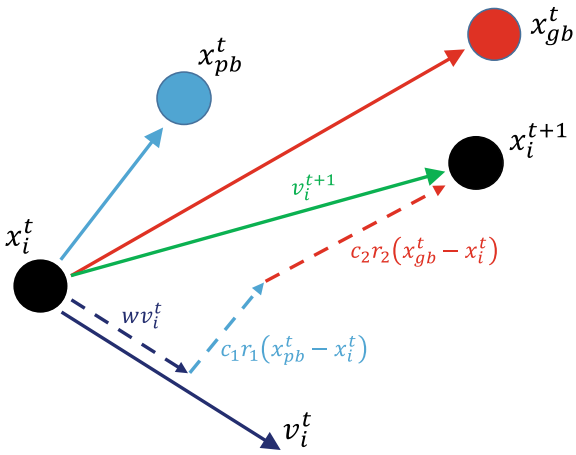

Fig. 2 Particle updating through the adjustment of velocity

terminating the loop, which performs Steps 2 and 3, may not let the randomness considered in velocity of particles help the algorithm discover new regions in the domain that may contain more optimal solutions.

3 Model Building

A three-storey model building was used to illustrate the proposed methodology developed to assess and minimize damage concentration in steel CBFs under seismic loading. The building selected is an office building located in Vancouver, BC on site Class C. The building measures 45 m × 45 m in the plan as shown in Fig. 3a. Four Moderately Ductile (Type MD) concentrically braced frames with chevron bracing located on the perimeter of the building are considered to resist lateral seismic loads in each direction of the building. One of the CBFs as shown in Fig. 3b is evaluated in this study. Columns are continuous along the height and are pinned at their base.

The loading calculation was performed in accordance with 2015 National Building Code of Canada [39]. The summary of gravity loads, including dead load, live load, snow load, and exterior wall load, are given in Table 1.

Lateral seismic loads were calculated using the equivalent static force procedure. The seismic-induced forces in the braces were then used to select brace cross-sections from ASTM A1085 Hollow Structural Sections (HSSs) following the Canadian steel design standard CSA S16:19 [5] provisions assuming a demand-to-capacity ratio of 0.5 or higher, which are considered as candidate braces to be fed into the algorithm as the optimization variables. An effective length factor $K = 0.9$ taking into account the effect of end connections was used to obtain the brace factored axial resistance. Braces with a broad range of demand-to-capacity and slenderness ratios help thoroughly investigate design alternatives. The candidate brace cross-sections are presented in Table 2.

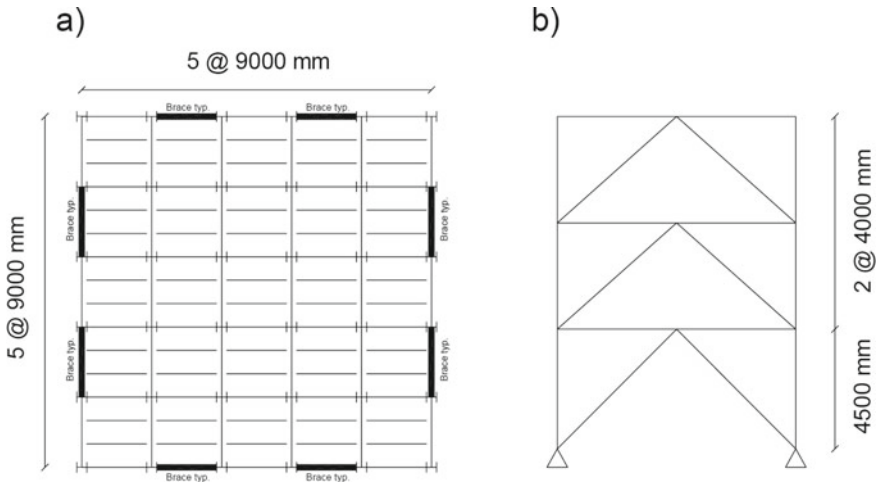

Fig. 3 **a** Plan view of building; **b** elevation view of frame

Table 1 Summary of gravity loads

Location	Source	Load kPa
Roof	Dead	1.35
	Snow	1.64
Floor	Dead	4.6
	Live	2.4
Exterior wall	Dead	1.5

The column and beams of the CBF are then sized with W-shape sections selected from ASTM A992 steel with the yield strength of 345 MPa following the capacity design principles. The CSA S16:19 provision associated with the reduction of the probable tensile resistance of the tension-acting braces in chevron braced frames lower than 4 storeys is ignored in this study to isolate the effect of the brace characteristics on the frame response.

Brace gusset plate connections were designed under probable axial tension and compression loads of the braces following the recommendations by [11].

4 Numerical Model

A fibre-based model of the frame was developed in the *OpenSees* programme [36]. The numerical model of the frame is shown in Fig. 4a. Columns, beams, and braces were modelled using nonlinear force-based beam-column elements with

Table 2 Candidate brace cross-sections for three-storey chevron CBF

Storey	Brace section	Area (mm^2)	KL/r	λ	Demand/capacity
3	HSS 5 × 5 × 1/4	2961.28	111.19	1.47	0.73
	HSS 5 × 5 × 5/16	3652.80	112.70	1.49	0.61
	HSS 5 × 5 × 3/8	4245.15	114.97	1.52	0.54
	HSS 4.5 × 4.5 × 1/4	2638.70	124.05	1.64	0.97
	HSS 4.5 × 4.5 × 5/16	3219.35	126.32	1.67	0.82
	HSS 4.5 × 4.5 × 3/8	3761.28	128.59	1.70	0.72
	HSS 4 × 4 × 1/2	4103.22	153.55	2.03	0.89
2	HSS 7 × 7 × 3/8	6180.63	79.42	1.05	0.63
	HSS 7 × 7 × 1/2	7999.98	81.69	1.08	0.50
	HSS 6 × 6 × 3/8	5212.89	93.79	1.24	0.91
	HSS 6 × 6 × 1/2	6683.86	96.82	1.28	0.74
1	HSS 8 × 8 × 1/2	9290.30	74.88	0.99	0.56
	HSS 7 × 7 × 3/8	6180.63	83.96	1.11	0.96
	HSS 7 × 7 × 1/2	7999.98	86.23	1.14	0.77
	HSS 7 × 7 × 5/8	9612.88	87.74	1.16	0.65

fibre discretization of the cross-section. Beams, columns, and braces were modelled according to recommendations by [17].

Shear-tab connections connecting beams to columns were modelled as pin-ended members. Relatively rigid elastic beam-column elements were used to model the portions of beams, columns, and braces that intersect with each other as shown in Fig. 4b. To reproduce brace out-of-plane buckling, assumed in design, gusset plate

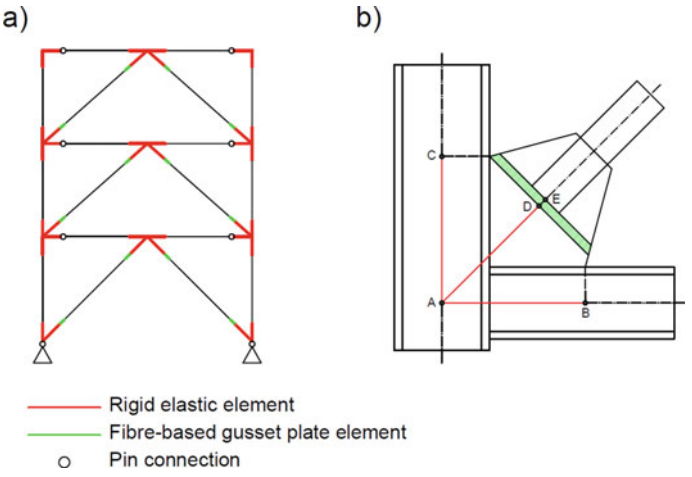

Fig. 4 Fibre-based numerical model of the frame: **a** three-storey CBF; **b** gusset plate connection

connections were modelled using a separate nonlinear beam-column element with fibre discretization of the gusset plate within the theoretical plastic hinge area, DE, shown in Fig. 4b, i.e. $2t$ offset where t is the gusset plate thickness.

All members were modelled using the *Steel02* material with properties recommended by [1]. The yield stress for brace cross-sections was set equal to 460 MPa, while the yield stress of 345 MPa was used for the rest of frame members.

To perform NonLinear Response History Analysis (NLRHA), masses were lumped at the mid-point and two ends of each beam. A leaning column, not shown in Fig. 4a, was modelled to account for P-Δ effects. Viscous damping was created using Rayleigh damping method consisting of initial stiffness of the frame CBF and seismic mass; the damping ratio ξ was set to 2% of critical damping.

5 CBF Design Optimization

5.1 Proposed Optimization Tool

An optimization tool was developed to improve the seismic response of steel CBFs by encouraging a uniform distribution of lateral deformations along the frame height. This tool was established by linking the PSO algorithm with the parametric *OpenSees* model of the CBF and incorporating a parametric design script capable of automatically designing beams, columns, and gusset plates. In the DCR minimization process shown in Fig. 2, the numerical model of CBF design alternatives plays the role of particles optimized by PSO algorithm, brace cross-sections are the optimization variables, *OpenSees* is the function evaluator to obtain objective function values, i.e. DCR, for each particle, and m is the total number of generations to be assessed by the optimization tool. Figure 5 details the steps followed by the automated tool developed to evaluate and minimize the drift distribution in steel CBFs. These steps are as follows:

1. First generation of frames is created by randomly selecting three brace cross-sections from the candidate brace list for each frame.
2. Beams and columns are sized using the lightest section available to carry brace probable tensile and compressive resistances plus gravity loads. This process is performed by a parametric design script.
3. Once beam, column, and brace sections are determined, gusset plate dimensions are calculated using the design script. Since the design script is directly implemented in the optimization tool, no penalty function is required for the PSO algorithm as all generated particles (i.e. braced frames) already belong to the feasible domain by satisfying all limit states addressed by design provisions.
4. Each frame is then modelled in *OpenSees* based on the selected beams, columns, braces, and gusset plates generated by the design script.
5. The NLRHA is performed using the numerical model in *OpenSees* for each frame and the respective DCR values are recorded.

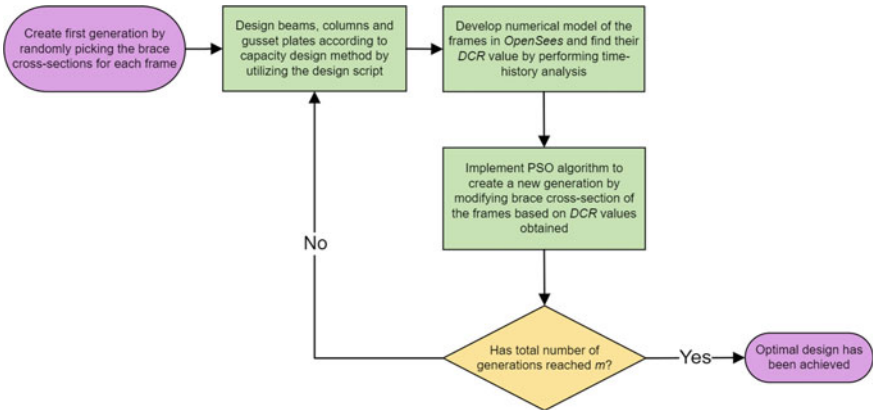

Fig. 5 Optimization workflow

6. At the end of each generation, the PSO algorithm modifies brace cross-sections for each frame based on DCR values obtained and creates a new generation.
7. Steps 2 to 6 are repeated until the termination criteria is met (i.e. number of generations analysed reaches m).
8. Last generation represents a potential set of design alternatives owing to the fact that all its particles have evolved generation by generation and possess relatively smaller DCR values compared to results obtained in previous generations. x_{gb}^{m} containing brace cross-sections of the frame with best performance (i.e. least DCR value) among all frames is reported as the optimum design.

5.2 *Clustering*

In order to further investigate and gain better understanding of the correlation between drift concentration and key attributes of brace cross-sections selected in the design stage, frames with desirable seismic performance obtained from the optimization tool can be classified into different groups based on the properties of their structural members and their lateral response features. K-means algorithm [31] is utilized to cluster the frames into k groups. The steps taken by this algorithm to partition the optimized frames are demonstrated in Fig. 6 and detailed below:

1. k random points in the domain of clustering problem are selected as centroids of clusters.
2. Euclidian distance between each particle (i.e. frame) and all centroids is measured. Frames will be assigned to the nearest centroid and form a cluster with it. Centroids remaining with no particles assigned to them are eliminated and the algorithm attempts to cluster the data into k-n groups, n being the number of centroids unable to attract any particles to their clusters.

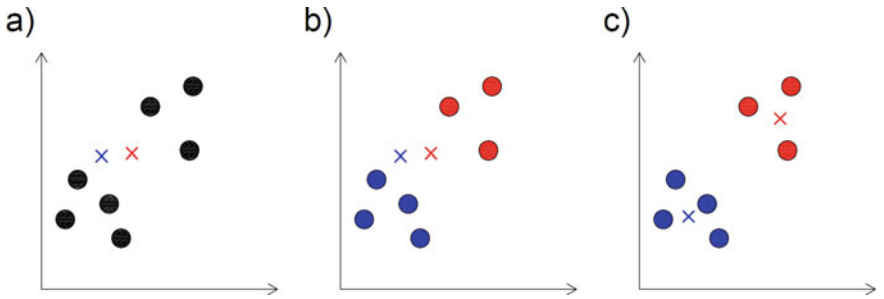

Fig. 6 K-means algorithm steps for clustering: **a** selection of random centroids, **b** particle assignment to centroids, **c** centroid adjustment

3. Each centroid's location is adjusted by moving it to the mean point of the particles inside the cluster it represents.
4. By repeating Steps 2 and 3, clusters are modified until particles assigned to each centroid do not change anymore.

Final clusters' shape is highly sensitive to the initial location of centroids. It is therefore suggested that this algorithm is performed on optimized frames multiple times until clusters with least variation between their particles are achieved. Finally, the closest particle to the centroid in each cluster can be reported as its representative.

6 Conclusions

This paper introduced a new methodology to address damage concentration in three-storey steel CBFs by implementing a metaheuristic optimization algorithm, namely the drift concentration ratios under lateral seismic loads are minimized. The proposed methodology is summarized as follows:

- A design script capable of sizing CBF braces, beams, columns, and gusset plates was developed and linked to a fully parametric numerical model constructed in the *OpenSees* programme.
- The PSO algorithm used in the proposed optimization tool generates numerous CBFs and modifies them iteratively with the objective of minimizing their DCR when the frame is subjected to earthquake ground motion accelerations.

- Candidate frames obtained from the optimization process with the respective least DCR value are finally grouped into different clusters using the K-means algorithm.

Although the current proposed methodology facilitates the seismic design of steel CBFs and assists structural designers to select safer structures less prone to concentration of lateral displacements under seismic loading, additional aspects of braced frame optimization need to be analysed as described below:

- The numerical model of shear-tab connections can be improved using elements with pinching material instead of assuming pin connections between beams and columns to account for the additional lateral stiffness and flexural strength provided by these connections towards the frame lateral response.
- Other steel CBF configurations such as Split-X (two-storey X) braced frames, which offer a more favourable solution when compared to chevron or V-bracing configuration, owing lesser unbalanced seismic load applied at the storey beam mid-span.
- Currently the optimization tool only varies brace cross-sections and the influence of beams and columns on the frame lateral response is evaluated indirectly. The number of optimization variables can be increased by creating separate optimization variables pertaining to beam and column sections to help take advantage of beam and column selections on controlling drift concentration.
- Other optimization algorithms such as genetic algorithm [15] or jEDE [6] can be used to discover most suitable algorithms for structural applications and achieve the algorithm with higher convergence rate and lesser function evaluation compared to the one used in this study.
- Multi-objective optimization can be implemented to account for other design parameters such as total weight of structure and its correlation with lateral response.
- Unsupervised algorithms capable of partitioning optimization results to different groups can be used to alleviate the need of determining the number of clusters k beforehand.

Acknowledgements This research is funded by the Natural Sciences and Engineering Research Council (NSERC) of Canada. The financial support is greatly acknowledged.

References

1. Ashrafi A, Imanpour A (2021) Seismic response of steel multi-tiered eccentrically braced frames. J Constructional Steel Res 181
2. Chen CC, Chen SY, Liaw JJ (2001) Application of low yield strength steel on controlled plastification ductile concentrically braced frames. Can J Civ Eng 28(5):823–836
3. Clark PW, Aiken ID, Kasai K, Kimura I (2004) Large-scale testing of steel unbonded braces for energy dissipation. In: Structures congress 2000: advanced technology in structural engineering, vol 103, pp 1–5

4. Clough RW, Huckelbridge AA (1977) Preliminary experimental study of seismic uplift of a steel frame. Earthquake Engineering Research Center, Report No. UCB/EERC-77/22
5. CSA (2019) CSA S16:19, design of steel structures. Canadian Standard Association, Toronto, ON, Canada
6. Cubukcuoglu C, Ekici B, Tasgetiren MF, Sariyildiz S (2019) Optimus: self-adaptive differential evolution with ensemble of mutation strategies for grasshopper algorithmic modeling. Algorithms 12(7):141
7. Deierlein G, Krawinkler H, Ma X, Eatherton M, Hajjar J, Takeuchi T, Kasai K, Midorikawa M (2011) Earthquake resilient steel braced frames with controlled rocking and energy dissipating fuses. Steel Constr 4(3):171–175
8. Eatherton MR, Hajjar JF (2014) Hybrid simulation testing of a self-centering rocking steel braced frame system. Earthquake Eng Struct Dynam 43(11):1725–1742
9. Eatherton MR, Ma X, Krawinkler H, Deierlein GG, Hajjar JF (2014) Quasi-static cyclic behavior of controlled rocking steel frames. J Struct Eng 140(11):04014083
10. Eberhart RC, Shi Y (2001) Particle swarm optimization: developments, applications and resources. Proc IEEE Conf Evolut Comput ICEC 1:81–86
11. Ebrahimi S, Mirghaderi SR, Zahrai SM (2019) Proposed design procedure for gusset plate dimensions and force distribution at its interfaces to beam and column. Eng Struct 178:554–572
12. Fahnestock LA, Sause R, Ricles JM (2006) Analytical and large-scale experimental studies of earthquake-resistant buckling-restrained braced frame systems. ATLSS Engineering Research Center, Report No. 06-01
13. Foutch DA, Goel SC, Roeder CW (1987) Seismic testing of full-scale steel building—part I. J Struct Eng 113(11):2111–2129
14. Ghersi A, Neri F, Rossi PP, Perretti A (2000) Seismic response of tied and trussed eccentrically braced frames. Proc Third Int Conf STESSA 2000:495–502
15. Goldberg DE (1989) Genetic algorithms in search, optimization and machine learning, 1st edn. Addison-Wesley Longman Publishing Co., Boston, MA, USA
16. Hassan OF, Goel SC (1991) Modeling of bracing members and seismic behavior of concentrically braced steel structures. Department of Civil Engineering, The University of Michigan, Ann Arbor, Michigan, Report No. UMCE 91-1
17. Hsiao PC, Lehman DE, Roeder CW (2012) Improved analytical model for special concentrically braced frames. J Constr Steel Res 73:80–94
18. Huckelbridge AA (1977) Earthquake simulation tests of a nine story steel frame columns allowed to uplift. Earthquake Engineering Research Center, Report No. UCB/EERC-77/23
19. Iami K, Yasui N, Umezu Y (1997) Development of tube-in-tube type FLD bracing member (force limiting device) and its impulsive analysis. In: Proceedings of the 1997 Structural Stability Research Council (SSRC), pp 515–533
20. Imanpour A, Tremblay R, Davaran A, Stoakes C, Fahnestock LA (2016) Seismic performance assessment of multitiered steel concentrically braced frames designed in accordance with the 2010 AISC seismic provisions. J Struct Eng 142(12):04016135
21. Iwata M, Kato T, Wada A (2000) Buckling-restrained braces as hysteretic dampers. In: Proceedings of the third international conference STESSA 2000, pp 33–38
22. Kelly JM, Tsztoo DF (1977) Earthquake simulation testing of a stepping frame with energy-absorbing devices. NZ Soc Earthquake Eng Bull 10(4):196–207
23. Kennedy J, Eberhart R (1995) Particle swarm optimization. In: Proceedings of ICNN'95—international conference on neural networks, vol 4, pp 1942–1948
24. Khatib IF, Mahin SA, Pister KS (1988) Seismic behavior of concentrically braced steel frames. Earthquake Eng Res Center 1:1–238
25. Kiggins S, Uang CM (2006) Reducing residual drift of buckling-restrained braced frames as a dual system. Eng Struct 28(11):1525–1532
26. Kim J, Choi H (2004) Behavior and design of structures with buckling-restrained braces. Eng Struct 26(6):693–706
27. Ko E, Tajiran F, Kimura I (2001) Building a safer future with unbonded brace. In: First international conference on steel & composite structures, Pursuan, Korea, pp 1549–1556

28. Lacerte M, Tremblay R (2006) Making use of brace overstrength to improve the seismic response of multistorey split-X concentrically braced steel frames. Can J Civ Eng 33(8):1005–1021
29. Lai J-W, Mahin SA (2015) Strongback system: a way to reduce damage concentration in steel-braced frames. J Struct Eng 141(9):04014223
30. Ma X, Deierlein G, Eatherton M, Krawinkler H, Hajjar J, Takeuchi T, Kasai K, Midorikawa M, Hikino T (2010) Large-scale shaking table test of steel braced frame with controlled rocking and energy dissipating fuses. In: 9th US National and 10th Canadian conference on earthquake engineering 2010, including papers from the 4th international tsunami symposium, vol 3, pp 1914–1923
31. MacQueen J (1967) Some methods for classification and analysis of multivariate observations. Proc Fifth Berkeley Symp Math Stat Probab 1:281–296
32. MacRae GA, Kimura Y, Roeder C (2004) Effect of column stiffness on braced frame seismic behavior. J Struct Eng 130(3):381–391
33. Mahin S, Lai JW (2008) An innovative approach to improving the seismic behavior of steel concentric braced frames. University of California, Berkeley, Proposal for SEAONC special projects initiative
34. Mar D (2010) Design examples using mode shaping spines for frame and wall buildings. In: 9th US National and 10th Canadian conference on earthquake engineering 2010, including papers from the 4th international tsunami symposium, vol 2, pp 1290–1299
35. Martini K, Amin N, Lee PL, Bonowitz D (1990) The potential role of non-linear analysis in the seismic design of building structures. In: Proceedings of Fourth US National conference on earthquake engineering, pp 67–76
36. McKenna F, Fenves G, Scott M (2000) Open system for earthquake engineering simulation. Pacific Earthquake Engineering Research Center (PEER)
37. Midorikawa M, Azuhata T, Ishihara T, Wada A (2006) Shaking table tests on seismic response of steel braced frames with column uplift. Earthquake Eng Struct Dynam 35(14):1767–1785
38. Morino S, Kawaguchi J, Shimokawa H (1996) Hysteretic behavior of flat-bar braces. Proc Int Conf Adv Steel Struct 2:1127–1132
39. NRC (2015) National Building Code of Canada (NBCC). Associate Committee on the National Building Code, Ottawa, ON, Canada
40. Perez RE, Behdinan K (2007) Particle swarm approach for structural design optimization. Comput Struct 85(19–20):1579–1588
41. Pollino M, Bruneau M (2010) Seismic testing of a bridge steel truss pier designed for controlled rocking. J Struct Eng 136(12):1523–1532
42. Pollino M (2015) Seismic design for enhanced building performance using rocking steel braced frames. Eng Struct 83:129–139
43. Popov EP, Ricles JM, Kasai K (1992) Methodology for optimum EBF link design. In: Proceedings of the 10th world conference on earthquake engineering, pp 3983–3988
44. Redwood RG, Lu F, Bouchard G, Paultre P (1991) Seismic response of concentrically braced steel frames. Can J Civ Eng 18(6):1062–1077
45. Rezai M, Prion H, Tremblay R, Bouatay N, Timler P (2000) Seismic performance of brace fuse elements for concentrically steel braced frames. In: Proceedings of the third international conference STESSA 2000, pp 39–46
46. Sabelli R (2001) Research on improving the design and analysis of earthquake-resistant steel-braced frames. NEHRP professional fellowship report. EERI
47. Sabelli R, Mahin S, Chang C (2003) Seismic demands on steel braced frame buildings with buckling-restrained braces. Eng Struct 25(5):655–666
48. Sause R, Ricles JM, Roke DA, Chancellor NB, Gonner NP (2010) Seismic performance of a self-centering rocking concentrically-braced frame. In: 9th US National and 10th Canadian conference on earthquake engineering 2010, including papers from the 4th international tsunami symposium, vol 2, pp 1280–1289
49. Stavridis A, Shing PB (2010) Hybrid testing and modeling of a suspended zipper steel frame. Earthquake Eng Struct Dynam 39(2):187–209

50. Torres A, Mahmoudi B, Darras AJ, Imanpour A, Driver RG (2022) Achieving an optimized solution for structural design of single-storey steel buildings using generative design methodology. In: Proceedings of the Canadian society of civil engineering annual conference 2021, CSCE21 structures track, vol 2, pp 301–312
51. Tremblay R, Degrange G, Blouin J (1999) Seismic rehabilitation of a four storey building with a stiffened bracing system. In: Proceedings of 8th Canadian conference on earthquake engineering, pp 549–554
52. Tremblay R (2000) Influence of brace slenderness on the seismic response of concentrically braced steel frames. In: Proceedings of the third international conference STESSA 2000, pp 527–534
53. Tremblay R, Lacerte M (2002) Influence of the properties of bracing members on the seismic response of concentrically braced steel frames. In: Proceedings of the 12th European conference on earthquake engineering, paper 481
54. Tremblay R (2003) Achieving a stable inelastic seismic response for multi-story concentrically braced steel frames. Eng J 40(2):111–129
55. Tremblay R, Merzouq S (2004) Dual buckling restrained braced steel frames for enhanced seismic response. In: Proceedings of passive control symposium, pp 89–104
56. Tremblay R, Poncet L (2004) Improving the seismic stability of concentrically braced steel frames. In: Proceedings—annual stability conference, structural stability research council, pp 19–38
57. Tremblay R, Bolduc P, Neville R, DeVall R (2006) Seismic testing and performance of buckling-restrained bracing systems. Can J Civ Eng 33(2):183–198
58. Tremblay R, Poirier L, Bouaanani N, Leclerc M, Rene V, Fronteddu L, Rivest S (2008) Innovative viscously damped rocking braced steel frames. In: Proceedings of the 14th world conference on earthquake engineering, paper no. 05-01-0527
59. Tsai KC, Lai JW, Chen CH, Hsiao BC, Weng YT, Lin ML (2004) Pseudo dynamic tests of a full scale CFT/BRB composite frame. In: Proceedings of the 2004 structures congress—building on the past: securing the future, pp 1241–1250
60. Uriz P, Mahin SA (2008) Toward Earthquake-resistant design of concentrically braced steel-frame structures. Pacific Earthquake Engineering Research Center, PEER Report 2008/08
61. Watanabe A, Hitomi Y, Saeki E, Wada A, Fujimoto M (1988) Properties of brace encased in buckling-restraining concrete and steel tube. Proc Ninth World Conf Earthquake Eng 4:719–724
62. Whittaker AS, Uang C-M, Bertero VV (1990) An experimental study of the behavior of dual steel systems. Earthquake Engineering Research Center, University of California, Berkeley, CA. Report UCB-EERC-88/14
63. Wiebe L, Christopoulos C, Tremblay R, Leclerc M (2013a) Mechanisms to limit higher mode effects in a controlled rocking steel frame. 1: Concept, modelling, and low-amplitude shake table testing. Earthquake Eng Struct Dyn 42(7):1053–1068
64. Wiebe L, Christopoulos C, Tremblay R, Leclerc M (2013b) Mechanisms to limit higher mode effects in a controlled rocking steel frame. 2: large-amplitude shake table testing. Earthquake Eng Struct Dyn 42(7):1069–1086
65. Wiebe L, Christopoulos C (2014) R = 100? Toward codification of controlled rocking steel braced frames. In: NCEE 2014—10th U.S. National conference on earthquake engineering: frontiers of earthquake engineering. Earthquake Engineering Research Institute
66. Yang C-S, Leon RT, DesRoches R (2008) Pushover response of a braced frame with suspended zipper struts. J Struct Eng 134(10):1619–1626